Stony Brook University

The official electronic file of this thesis or dissertation is maintained by the University Libraries on behalf of The Graduate School at Stony Brook University.

Fluorescent DNA-templated silver nanoclusters

A Thesis Presented

By

Ruoqian Lin

to

The Graduate School

in Partial Fulfillment of the

Requirements

for the Degree of

Master of Science

in

Materials Science and Engineering

Stony Brook University

May 2014

Stony Brook University

The Graduate School

Ruoqian Lin

We, the thesis committee for the above candidate for the

Master of Science degree, hereby recommend

acceptance of this thesis.

Dmytro Nykypanchuk – Thesis Advisor
Staff scientist, Center for Functional Nanomaterials at Brookhaven National
Laboratory

Jonathon Sokolov – Committee Member
Professor, Material Sciences and Engineering

Dong Su – Committee Member
Staff scientist, Center for Functional Nanomaterials at Brookhaven National
Laboratory

This thesis is accepted by the Graduate School

Charles Taber
Dean of the Graduate School

Abstract of the Thesis

Fluorescent DNA-templated silver nanoclusters

by

Ruoqian Lin

Master of Science

in

Materials Science and Engineering

2014

Because of the ultra-small size and biocompatibility of silver nanoclusters, they have attracted much research interest for their applications in biolabeling. Among the many ways of synthesizing silver nanoclusters, DNA templated method is particularly attractive—the high tunability of DNA sequences provides another degree of freedom for controlling the chemical and photophysical properties. However, systematic studies about how DNA sequences and concentrations are controlling the photophysical properties are still lacking. The aim of this thesis is to investigate the binding mechanisms of silver clusters binding and single stranded DNAs. Here in this thesis, we report synthesis and characterization of DNA-templated silver nanoclusters and provide a systematic interrogation of the effects of DNA concentrations and sequences, including lengths and secondary structures.

We performed a series of syntheses utilizing five different sequences to explore the optimal synthesis condition. By characterizing samples with UV-vis and fluorescence spectroscopy, we achieved the most proper reactants ratio and synthesis conditions. Two

of them were chosen for further concentration dependence studies and sequence dependence studies. We found that cytosine-rich sequences are more likely to produce silver nanoclusters with stronger fluorescence signals; however, sequences with hairpin secondary structures are more capable in stabilizing silver nanoclusters.

In addition, the fluorescence peak emission intensities and wavelengths of the DNA templated silver clusters have sequence dependent fingerprints. This potentially can be applied to sequence sensing in the future. However all the current conclusions are not warranted; there is still difficulty in formulating general rules in DNA strand design and silver nanocluster production. Further investigation of more sequences could solve these questions in the future.

To my parents

Table of Contents

List of Figures

Acknowledgement

First, I want to thank my advisor Dr. Dmytro Nykypanchuk for his guidance and mentorship. From a student who knows nothing about scientific research when first joined his group to a competent researcher who can compile a complete thesis, I have learned every bit of the knowledge and techniques from him. His rigorousness and talents have and will bound and inspire me throughout my academic career.

Second, I want to thank my committee members—Professor Sokolov and Dr. Dong Su—for spending their invaluable time on reading my thesis. I am in debt to them.

Third, I want to think my parents who have unlimitedly supported me for every decisions I made. Choosing an academic career path is a difficult one and I sincerely thank them for respecting me.

Last but certainly not the least, I want to thank my friends and colleagues at CFN—Jing Li ("Hua Hua"), Ye Tian, Wenyan Liu, Fang Lu, Yugang Zhang—for their help and support. Without them, my life at CFN would be miserable.

Chapter 1 Introduction

The development of high quality fluorophores has revolutionized imaging of biological organisms at the molecular scale. All fluorophores can be categorized into three main classes. The first class is the well-studied and most commonly used fluorescent dyes. They are versatile and low price and they are comparatively easier to be synthesized; however, they usually suffer the problem of quick photobleach. The second class is semiconductor quantum dots. They are considered to be more stable in terms of photostability and they have higher fluorescence intensity as a result of high molar coefficient. However, all these properties rely on the surface protection of quantum dots which is not easy to control. The third class of fluorophores is silver nanodots. They are a new class of fluorophores that are much smaller than quantum dots; yet their photophysical properties are highly competitive with those of quantum dots. In addition, these silver nanodots can be template by DNAs. The high tunability of the DNA sequences provides another degree of freedom for controlling the fluorescence properties. However, how DNA sequences and concentrations are modifying the photophysical properties have not been studied systematically. Here, in this thesis, we report synthesis and characterization of DNA template ultra-small silver nanoclusters and we provide a systematic interrogation of the effects of DNA sequences and concentrations.

1.1 Current Status of Fluorophore Science

There is a long history of the study and application of organic fluorescent. They are most frequently used as sensors in optical chemistry and organelles imaging. Using organic dyes, we are provided with means for detecting selected ions or electrically neutral species including the information of their location, activities or concentrations (*1*). A wide range of organic fluorophores are available for biological labeling, and many new fluorophores are under development. In 2003, several novel fluorophore for single molecule imaging were reported by Katherine A Willet's group(*2*) . They, however, without exception, suffer from rapid photobleaching. It has been shown that before photobleaching, a single organic dye molecule can only emit approximately 10^6 photons. Currently, a lot of attention has been paid to developing near-infrared (NIR) emitting fluorophores with high photostability and selectivity .
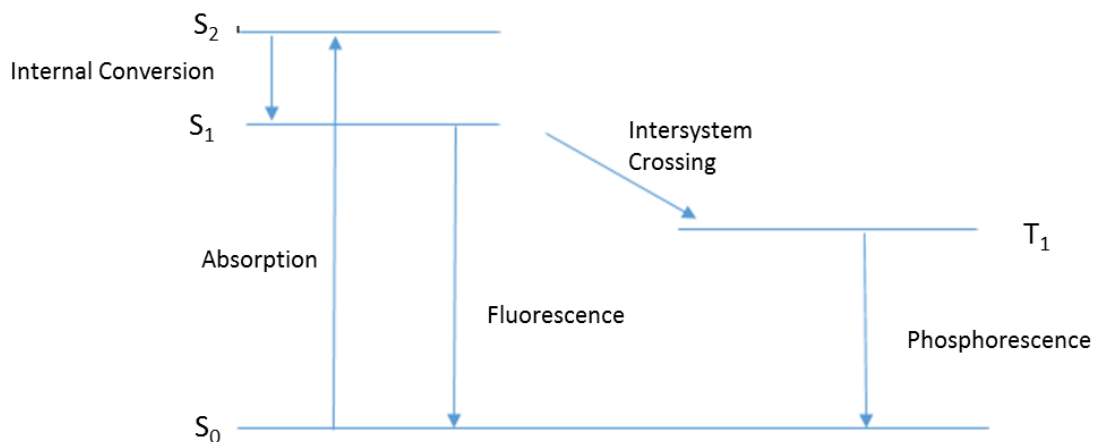
Figure 1 The Jablonski diagram describing the energetic processes of fluorescence.
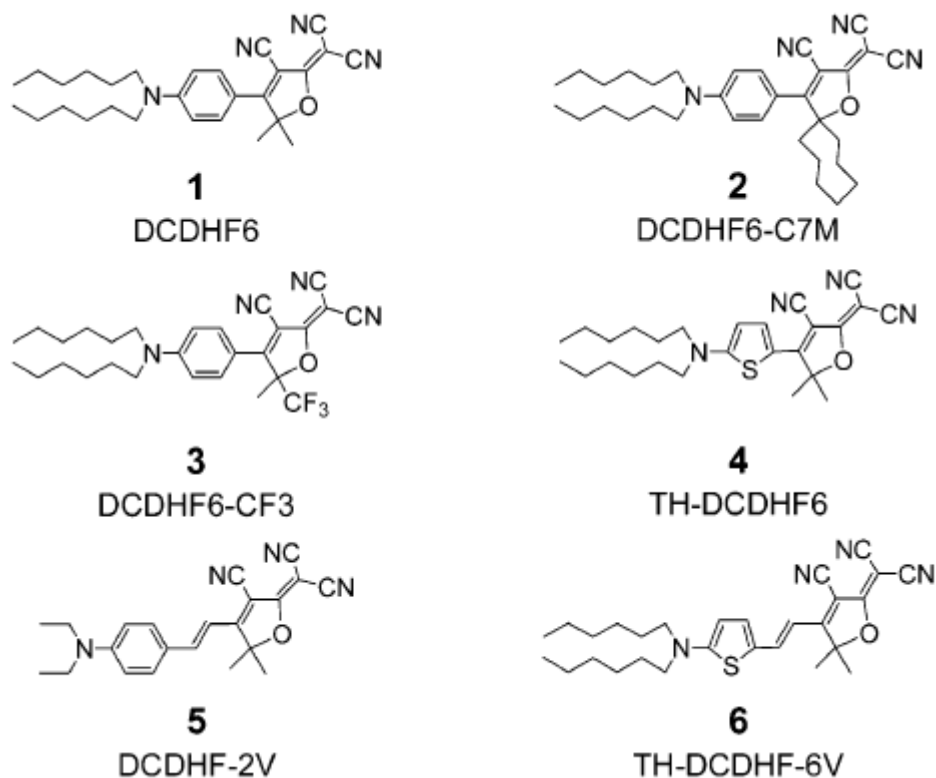
Figure 2 Molecular structures of the fluorescent organic dyes. Figures adapted from ref. (*2*)

.

Compared to organic fluorescent dyes, semiconductor quantum dots are much more photostable, typically, for a single molecule, emitting 10 times more photons than organic dyes before bleaching (*3*). On the other hand, most of the photophysics properties behave as a function of particle size, which is often effected by the surface protection (*4*). With the decrease of particle size, the gaps between energy levels are observed to increase. Based on the emission spectra of single QD, Blaton et al.(*5*) and Nirmal et al (*6*)found many exciting properties of single semiconductor QDs, most of which disappear when there is an aggregation of many QDs. The large particle sizes are often responsible for the barriers in molecular labelling.

Silver nanoclusters act as the most recent class of fluorophores with similar photophysical properties to those of semiconductor QDs, but what is different is that they have much smaller overall sizes. Silver nanoclusters, also named as silver nanodots or silver quantum dots. Up to now, some experiments have shown the fact that silver nanoclusters have superlative photostability, including constant emission rates, and brightness (7). Even if in biological fluids, the photobleaching rate of them is quite low. In this way, especially when protected by oligonucleotides, they have longer lifetime which is usually at nanosecond scale. With larger molar extinction coefficients and short triplet state residences (Figure 1), silver nanodots show strong emission intensity and molecular brightness which overwhelm organic dyes a lot. In addition, in terms of two-photon absorption cross sections, silver nanoclusters have almost 100-fold enhancement over those of organic dyes. However, to date, it is still difficult to get a lot of spectrally pure emitters.

1.2 Protection Groups for silver nanoclusters

1.2.0 Synthesis of silver nanoclusters

Since silver nanoclusters are stable in aqueous environment, it is not difficult to synthesis them via chemical or photoactivation method(8)(Figure 3). Up to now, the most widely-used method is to mix silver ions with an organic protection group, then reduce the silver ions by photactivation or chemical reduction. Although some spectrally pure silver nanoclusters have already been prepared in this way, it is still a great challenge for us to

prevent these nanoclusters from aggregation, which is favored in terms of thermodynamics. At the same time, the strong tendency of silver nanoclusters to oxidation is another important factor that effects their stability. Unless they are encapsulated kinetically or separated in inert rare gas matrices, silver nanoclusters show the expected emission.

Taking these two important factors into consideration, it is quite necessary to introduce reasonable protection groups to improve both stability and photophysical properties of silver nanoclusters, and prevent the formation of nanoparticles. Four protection groups are mainly used as scaffolds now, which are solid matrices, polymer, peptide and DNA.
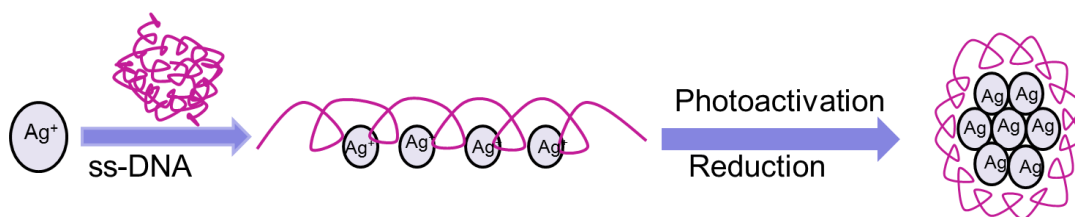
Figure 3 Illustration of the creation of silver nanoclusters.

1.2.1 Solid matrix protected silver nanoclusters

As a scaffold to trap silver nanodots, solid matrices also protect nanodots from agglomeration and oxidation. Noble gas matrices(*9*), glasses(*10*), and zeolites(*11*) are the three most known scaffolds, and they are all able to restrict diffusion and aggregation. Unfortunately, they still cannot guarantee a uniform size of all the clusters.

Among the above three scaffolds, species trapped by noble gas matrix are studied most intensively, such as Ag_1, Ag_2, Ag_3, Ag_4, which are according to stoichemistry[12, 13]. Most of these silver clusters have very strong UV absorption. In addition, there is a correlation between UV absorption and cluster sizes or geometric formation. Emitters with emission at longer wavelength are regarded as the result of Ag_3. For example, an emitter has been found, which has emission at 560nm with excitation at 514nm, 458nm, 421nm and 364nm[13]. Although initial stoichiometry is well controlled during preparation, as is shown in the spectral, it is very likely that there is post-isolation agglomeration, which brings difficulties in spectral assignments. Because of the existence of large Stokes' Shift, increasing of cluster size does not necessarily mean a red shift of the fluorescence peak. For instance, Ag_4 shows an intensity peak at 458nm when excited at 405nm or 387nm[14]. Although there is few reports about clusters larger than Ag_4, Ag_8 has been reported to show an obvious emission at 321nm with a shoulder at 318nm, when it is excited at 312nm[15].

As is known, thermal, chemical and photo-reduction make it possible for silver nanoclusters to be formed on microcrystal surfaces. For example, in the field of film-based image storage, silvers clusters can be trapped on silver halide microcrystals[16]. However, these species are only stable and show fluorescence at very low temperature, below -150℃ or so. Three main emission peak at 550nm, 590nm and 640nm show up in the emission spectra with a peak at 440nm in the excitation spectra. Later report in 2001 indicated that some of such surface-trapped silver nanoclusters can show high emission intensity at room temperature[17], and that is to say, Ag clusters could be a kind of

encouraging material used in the field of biology, chemistry or material engineering. For AgBr, the oxidized surfaces are reduced by photo-dissociation ($2AgO+2hv{\rightarrow}2Ag+2O{\bullet}$), and silver atoms are formed on the surfaces. Also, with the help of photoreductants, silver nitrate solution can be a source of silver nanoclusters. Although it is not difficult to get silver clusters in this way, quick aggregation into larger nanoparticles result in the loss of fluorescence.

1.2.2 Synthetic polymer-protected silver nanoclusters

Silver nanoclusters based on solid matrices can be used as fluorescent materials, or for information storage. However, those silver clusters that can be used as fluorophore for biolabeling must be water-soluble and stable. Water-soluble clusters have been prepared with dendrimers, although these species usually lack flexibility or stability.

As reported, Henglein has used poly(phosphate) to protect silver clusters in the aqueous environment of $AgClO_4$ with γ-irradiation(*18*). Later, Mostafavi et al. used another polymer, poly(acrylic acid) (PAA) as the protection group(*19, 20*). At different pH condition, different absorption peaks appear which correspond to different complexes, but no fluorescence emission was got. At least, these results indicated that polymer-protected silver clusters can be kept in aqueous solution, and may show fluorescence with some specific methods. Therefore more people investigated other relevant synthesis methods.

Instead of using γ-irradiation, photo-reduction is also a good idea to reduce silver ions. Zhang and others used silver ions and acrylic acid with hydrogels at a [Ag+]/[-COOH] ratio of 1:1 to get silver clusters after photo-reduction(21). The solution was irradiated at 365nm, and with the time goes on, the color of the solution became darker, from light pink to dark red. Also, the absorption changed in the spectra. Comparing the absorption and emission peaks, it is not difficult to find that not all the species can emit fluorescence. Continuous photo-reduction caused an aggregation of silver nanoparticles which result in the emission intensity increase and then decrease gradually.

Shen et al. used similar method with much more complicated polymer to get a kind of more stable silver nanoclusters(22). The multiarm polymers they used shows a core/shell structure which means the density of acrylic acid changes gradually from core to shell. And this makes it possible to trap more silver ions inside because of the cage effect. What's is different in this case is that continuous long time irradiation does not change the emitters a lot, although there are still more than one emitter. Arm length is a very important factor in the control of emission wavelength of these emitters. The limited data showed shorter-arm polymers produce emitters at shorter wavelength. In addition, lower carboxylic group density may cause a poorer ability to generate silver nanodots. Recently, a commercial polymer, poly(methacrylic acid) (PMAA) was used as another new scaffold for silver nanoclusters(23). Similarly, a few emitters are produced under this synthesis condition. But some special photophysical properties are observed, typically, a shorter fluorescence lifetime of 2.3ns and higher quantum yield of 19%.

To get rid of silver nanoparticles, visible light was utilized to photo-reduce the mixture of silver ions and PMAA. With different polymer concentration, samples usually show different absorption and emission wavelength. In general, there is a red shift observed when the silver/ methacryclic acid (Ag/MAA) is increased(*24*). However, up to now, there is still not enough evidence to show whether this is a result of different structure formed or not. There is a high possibility that the shift is caused by the micro-environments which is directly affected by the local polymer concentration. Both initial Ag/MAA molar ratio for synthesis or additional free polymer can result in such different environment(*24*). All these obvious phenomena indicate that the binding between silver nanoclusters and polymer is very flexible, and it is easy for the silver nanoclusters to form again when exposed to excessive polymers. At some specific higher concentration, the clusters show longer lifetime of hundreds of micro-second, compared with nanoseconds mentioned before.

Another lower molecular weight polymer, PAA, also acts as a good protection group in the formation of silver nanoclusters(*23*). By adding PAA before chemical reduction by sodium borohydride, strong luminescence intensity is able to be successfully maintained compared with that without PAA(*25*)(Figure 4). Based on the current results, we find it is more likely for a polymer to stabilize silver nanoclusters when it contains PAA fragment. These advantages may due to the strong interaction between carboxylic acid and silver ions. On the other hand, too strong such interaction may interfere the formation of silver nanoclusters. In addition, even with the formation of ultra-small clusters, the

problem of Stokes shift, poor chemical and physical stability etc. have not been solved

yet.
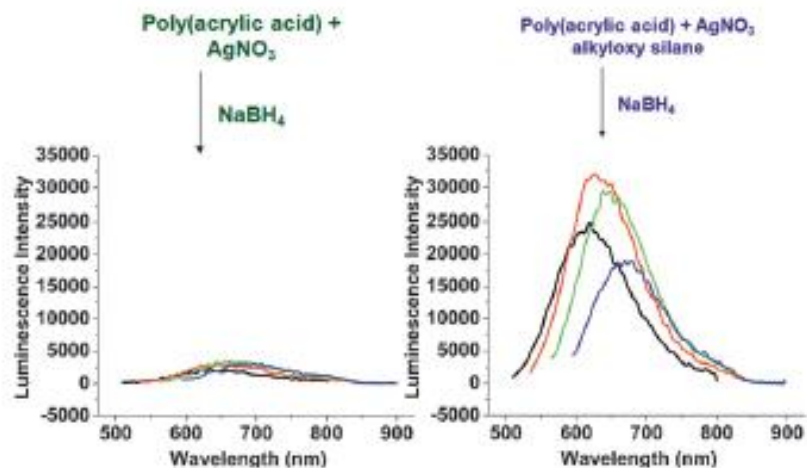
Figure 4 Poly(acrylic acid) protected silver nanoclusters. The emission intensity is greatly enhanced when alkyloxy silane is utilized to chelate silver ions before chemical reduction. Figure adapted from ref. (*25*)

1.2.3 Peptide-protected silver nanoclusters

Peptides or proteins share the same character that contain carboxylic acids as PAA, which

lead them a strong combination with silver ions. However, the different residues in the

protein sequence make a particular local environment to change the silver nanocluster

stability.

Baskakov group first reported the enhancement observed of the fluorescence of thioflavin

T with reduced silver(*26*). When thioflavin T is mixed with silver ions in solution, the

fluorescence of thioflavin T first decreased and then increased under 330nm light

irradiation. This phenomenon may be explained as a result of photoreduced silver clusters which have free surface plasmon electrons that can enhance emission rates. Although an enhancement was observed, no other emission peaks appeared. In contrast to this, there was another story when the thioflavin T silver complex was applied on the cover slip surface to stain amyloid fibrils. New emission peaks showed up which ranged from green to red, and most of these emitters are quite stable. Currently, the obvious difference between the spectra of thioflavin T silver hybrids in solutions and in amyloid fibrils indicates protein do play an important role as template, though nobody has found out clearly the mechanism of it.

Cajal's study on the utility of silver ions as staining agents for neurofibrils and nuclear subcompartments was the pioneer in this field(*27*). Inspired by the strong affinity between silver ions and argyrophilic proteins, several short designed peptides were further investigated(*28*). These specific designed proteins contains a series of regular amino acids: glutamic acid (15.6%), lysine (12.7%), and aspartic acid (8.5%). A15-residue peptide has been found to be useful in stabilizing fluorescence of silver clusters exposed in phosphate buffered saline (PBS) which is produced by chemical reduction of peptide and silver nitrate. Another set of experiments show the tendency that more hydrophobic residues in the longer sequences may lead to a longer chemical lifetime, especially at room temperature. For example, compared with short sequences which only maintain 3-day stability, these two sequences: HDCHLHLHDCHLHLHCDH and HDCNKDKHDCNKDKHDCN, were able to extend the lifetime of clusters to several weeks.

Another protein called bovine pancreatic R-chymotrypsin was also used as a protection group to stabilize silver nanodots(29), which were produced by reducing mixture silver nitrate and the protein with sodium borohydride in degassed aqueous solution. Similarly, the silver clusters have a red emission. However, the high resolution TEM indicates that the mixture is not pure nanocluster, but contains some 1nm nanoparticles. But current results have not elaborated the correlation between particle or cluster sizes and photophysical properties.

1.2.4 DNA protected silver nanoclusters

Introduction

Nowadays, there's an argument that DNA-templated silver nanoclusters are the most outstanding encapsulated silver clusters due to their patent photophysical properties which are the result of strong affinity between deoxyribonucleic acid and silver ions. Especially, the cytosine base show the strongest binding with silver ions, which even makes it possible for silver ions to stabilize cytosine-cytosine pair(30). In addition, the properties of being brighter, more photostable and more quantifiable make DNA encapsulated silver nanoclusters to be a good potential choice as biological sensor or stain in the future application.

Functions and their underlying mechanisms

Silver ions can bind successfully to heterocyclic base rather than phosphate or sugar groups when mixed with DNA sequences with high selectivity. Up to now, the most

popular way to synthesis DNA-templated silver clusters is to reduce silver ions which are mixed with DNA oligonucleotides via chemical reduction by sodium borohydride (Figure 3). After such chemical reduction, silver atoms are supposed to bind to some specific bases of oligonucleotide tightly, which make the whole system to be stable. DNA sequence and structure design is not only regarded as a key factor in the stabilization of AgNCs, but also in controlling their fluorescence properties. Fine-tuning the DNA sequences including the length, bases and secondary structure can result in different emitters in the range of visible to near-IR(*31*).

Synthesis

DNA stabilized silver nanoclusters were first successfully synthesized in phosphate buffer by Dickson's group in 2004(*32*). The single strand they used as the template is 5'-AGGTCGCCGCCC-3'. However, what they got is more reasonable to be regarded as a mixture of emitter whose optimum excitation and emission wavelengths are different. Such formed silver nanoclusters usually contain less than 4 silver atoms, and have a lifetime in nanosecond scale. Based on the density function calculations, they indicated that silver atoms highly prefer to bind with cytosine bases compared with other bases (Figure 5), and the binding between thymine and silver atoms is the weakest. Although in terms of electrostatic interaction, it is very likely that phosphate ions on DNA backbones combine strongly with silver cations, the fact is quite different from the expectation. According to the pH study of the synthesis condition, they suggest that N3 on cytosine ring is the main interaction site with silver ions. At the same time, silver atoms are

thought to be able to make the mismatch of cytosine-cytosine in DNA duplexes more stable.
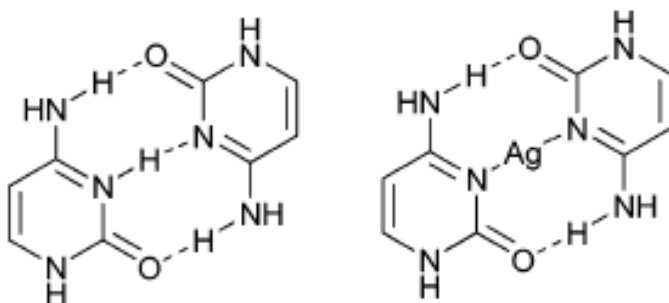
Figure 5 Model of i-motif-like structures with silver ions.

Dickson's and Petty's groups believe that in the process of back-electron transfer, DNA provide a charge-accepting location which is photostable and photaccessible. The nanosecond fluorescence of silver nanoclusters is likely due to the transfer of photoinduced charge from silver nanoclusters to the single strand DNA bases(*32*).

Since cytosine is the most favorable binding site, Petty et al. reported that 12-mer polycytosine (C_{12}) is another choice for encapsulating template(*33*). From the fluorescence and absorption spectra, they indicated that multiple clusters were formed which vary from 2 Ag atoms to 7 Ag atoms. The cluster shows primarily a red emission, while there are also blue emission and green emission. With the time goes on, the intensities of blue and green emissions increase, while the intensity of red emission decrease. In addition, an isosbestic point is showed in the emission spectrum, which implies that the species with red emission transfer to blue and green emission species.

14

The mixture formed with C_{12} can be purified in PBS to get a red emitter. Except for C_{12}, 20-mer oligocytosine (C_{20}) and other cytosine-rich sequences can also protect silver nanoclusters(*34*).

The fluorescence emission wavelength and stability is highly sequence dependent. Richard and others used five different single strand DNA sequences as scaffolds to synthesize five different pure Ag NCs(*31*), whose emission wavelength varies from visible to near-IR. Blue and green emitters could only be got in unbuffered condition, and lacked photostability. On the other hand, the yellow, red and near-IR emitters could be created in buffered solutions, and are more stable. Martinez's group used four long DNA strands to adjust Ag NCs' emission, both sequence and length of which are different(*35*). These species emitted from green region to near-IR region with different quantum yields. The photostability and chemical stability of these silver nanoclusters are effected by the storing temperature and salt concentration in the solutions. Unfortunately, up to now, designed and sequence-specific emissive silver nanoclusters have not been achieved.

Except for the fact that distinct bases affect the local concentration of silver nanoclusters, DNA secondary structure also greatly influence the creation of silver nanoclusters. For example, compared with the normal C_{12} sequence, a similar sequence inserted with 4 more bases at the end, which enables it to form a hairpin structure, increased the quantum yield of the previous yellow emitter(*31*). Dickson's group found that DNA hairpin sequences help a lot in improving stability, quantum yield and spectral purity of silver nanoclusters.

Gwinn's group made a further step in this direction. They used C-strand (5'-TATCCGTC$_5$ATAGGCA-3') and G-strand (5'-TGCCTATG$_5$ACGGATA-3') (Figure 6) to hold Ag nanodots to get higher intensities at 648nm and 646nm(*36*). Opposite from what is widely known, DNA hairpin, which is considered to be relatively inflexible structure, is able to improve fluorescence brightness of Ag NCs. Later, a series of hairpin structures with homopolymers of one of the four bases in single-stranded loops have been developed. These so-called C loop, G loop, A loop and T loop are hairpin oligomers, and they partially complement with themselves. Silver clusters encapsulated with C-loop and G-loop show more than 10 times stronger fluorescence than those in A-loop and T-loop. And the fluorescence of C-strand and G-strand solution are a little bit stronger than C-loop and G-loop. However, the double-stranded DNA sequence of C strand and G strand doesn't show obvious fluorescence as sing-stranded ones, although there are attached silver atoms. Probably it is because that the Waston-Crick pairing prevent the Ag atoms from the regular specific binding sites where silver nanodots show fluorescence(*36*). In addition, DNA secondary structure influences the chemical yield of fluorohpores and fluorescent emission wavelength.
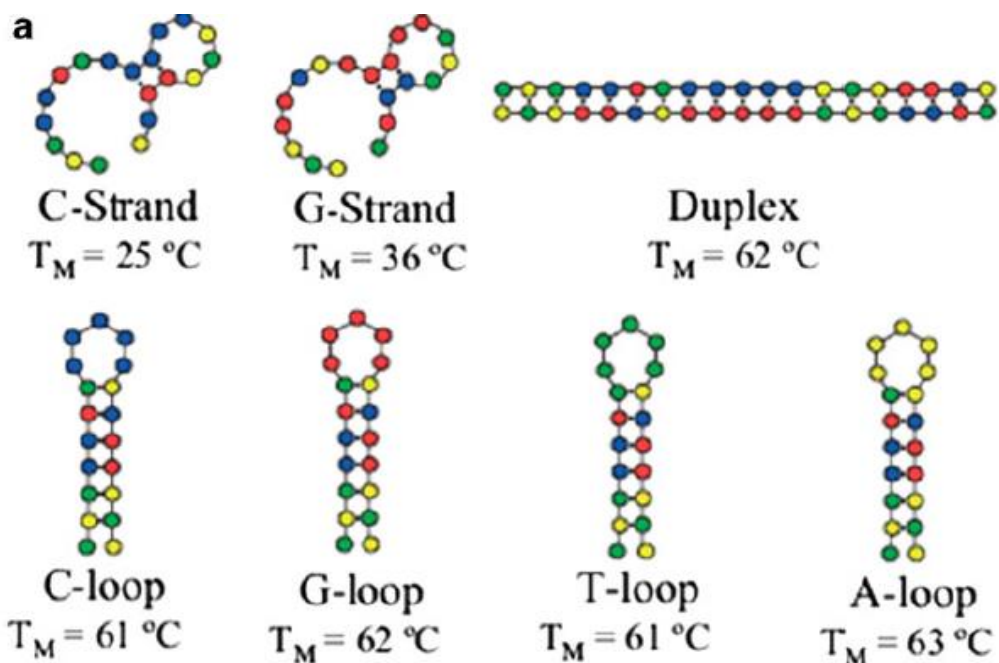
Figure 6 19-base DNA oligomers used by Gwinn's group. Figure adapted from ref(*36*).

Another factor that influences the production of silver nanoclusters is the Ag/base ratio. Usually, the optimal nucleobase: Ag ratio is 2:1(*34, 36*). With the increase of this ratio from 2 to 2.7 or larger than 3, most emissive species transforms to purer emitters at a longer wavelength. For instance, when the nucleobase: Ag ratio is 2:1, 20-mer polycytosine produces red emitters. And with increase of nucleobase, the red emitter transforms to a more stable green emitter in two days. What's more, both solvent evaporation and ethanol precipitation can concentrate these DNA-templated silver nanoclusters without destroying them.

Characterizations

Fluorescence measurements

Fluorescence measurement is the most important and primary method used in silver nanocluster characterization. Generally, people want to record both excitation and emission spectra of different fluorophores. What an emission spectrum is the distribution of emission wavelengths, measured at a constant excitation wavelength. At the same time, an excitation spectrum show the dependence of emission intensity on the excitation wavelength at a constant emission wavelength. With excitation into higher electronic and vibrational levels, the excited molecules quickly release excess energy, leading the fluorophore into the lowest vibrational level of S_1 (Figure 1). Because the fast relaxation, for most fluorophores, there is no direct correlation between the excitation wavelength and quantum yields, or emission spectra. However, there are some exceptions, such as fluorophores having two ionization states, and each of them displays various absorption and emission spectra. Also, some molecules can emit from S_2 level, which this phenomena is quite rare, especially in the field of biological and biochemistry.
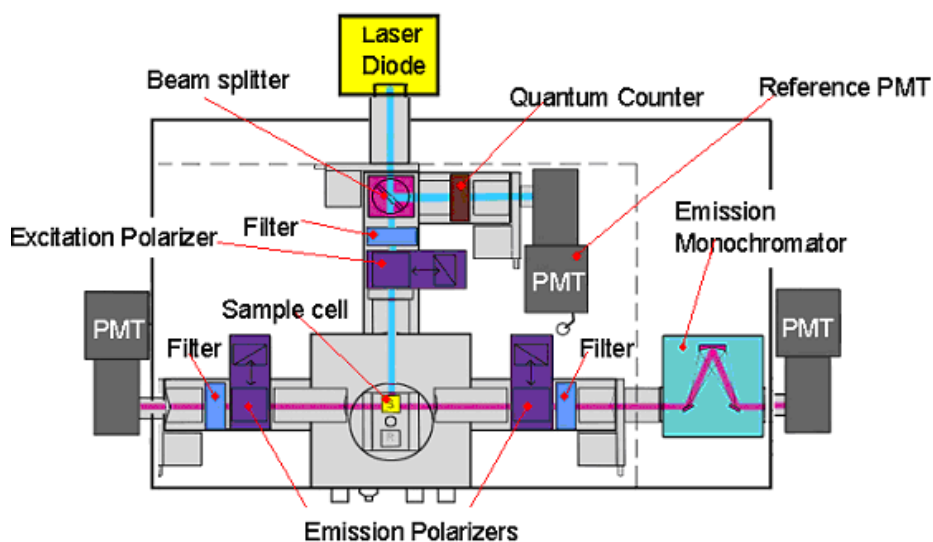

Figure 7 Schematic diagram of a spectrofluorometer. Figure adapted from wikipedia

For example, Petty's group collected a set of fluorescence spectra about the silver clusters templated with dC_{12}. In this specific case, fluorescence spectra behave as a function of excitation wavelengths(*37*). Several bands are observed at four different excitation wavelengths (Figure 8), including a strongest emission peak at 665nm, when excited at 580nm, and three other weaker emission peaks, corresponding to three different excitation wavelengths. These distinct bands should correspond to several electronic transitions. With a time dependent study, they found the bands increase and then decrease. The two peaks excited at 580nm and 280nm have quite similar emission wavelengths, which suggests that they are corresponded to a same electronic state of a same emitter. In Figure 9, it is easy to see an isosbestic point, which is a good evidence to support the conclusion that there is a chemical interaction between blue/green and red emitters. Also, they made a comparison between sample with extra Ag^+ and sample with extra BH_4^-. With additional BH_4^-, the blue/green emission completely disappear, and the red emission increase with a blue shift. They suggested that the shift may be the result of the partially overlap of two species in this spectral region.
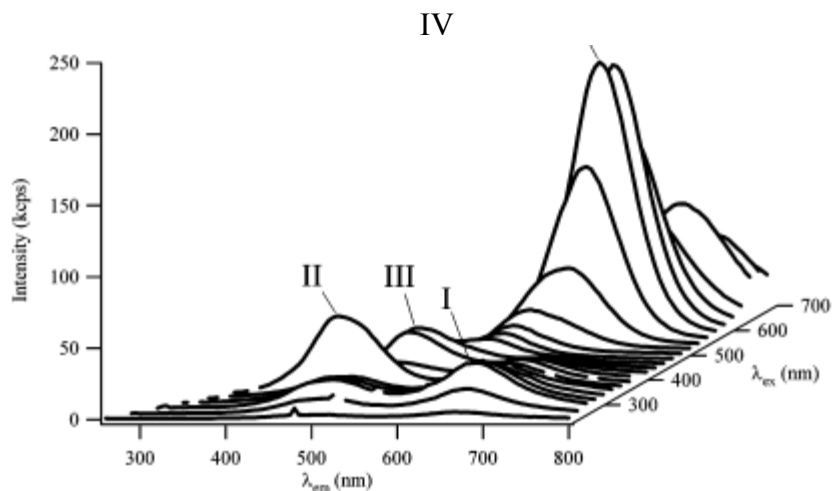
Figure 8 Fluorescence emission spectra as a function of excitation wavelengths, which was measured every 20nm from 240nm. Figure adapted from ref. (*37*)
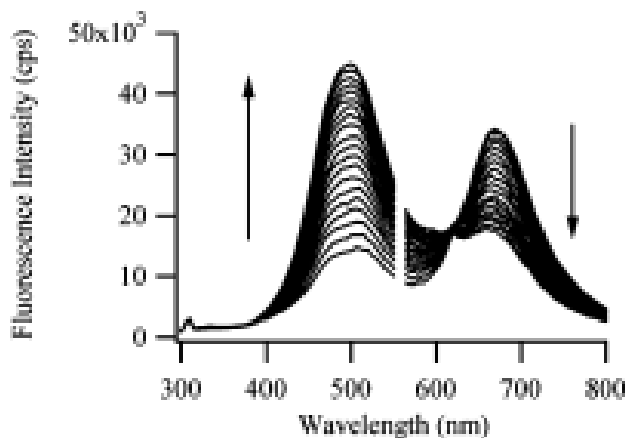
Figure 9 Time evolution of the fluorescence emission spectrum excited at 280nm. Figure adapted from ref.(*37*)

At the same time, a lot of effort has been paid to sequence-dependt fluorescence study. People try to get spectral purer, fluorescence stronger emitters. Richard et al. collected both excitation and emission spectra of five various Ag NCs using five different ssDNA as template(Figure 10), which range from visible region to near-IR region(*37*).
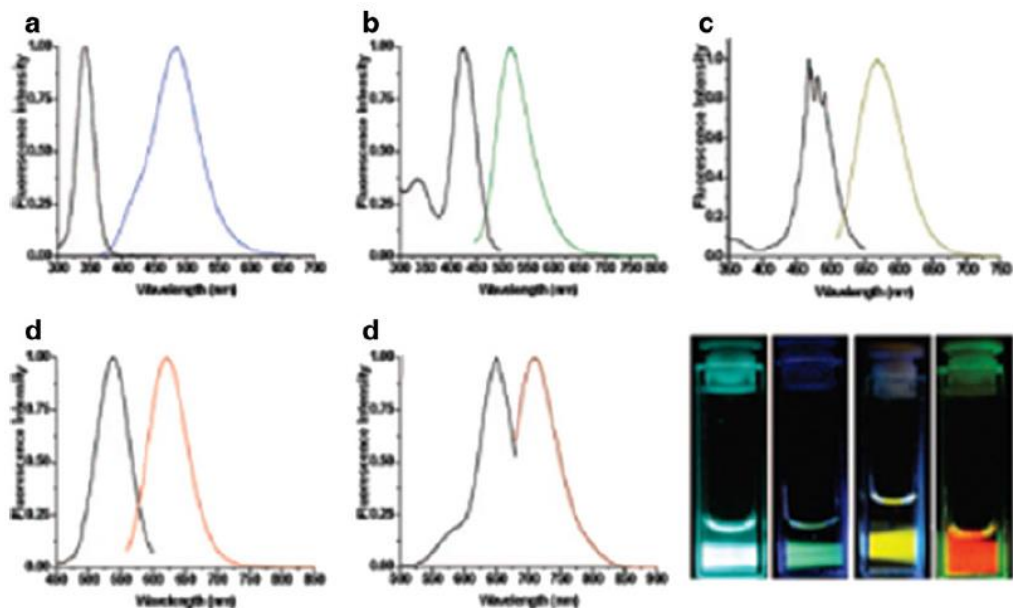
Figure 10 Excitation and emission spectra for five different single stranded DNA-templated silver nanoclusters. (a) Blue emiiters created in 5'-CCCTTTAACCCC-3', (b) green emitter created in 5'-ccctcttaaccc-3', (c) yellow emitters created in 5'-CCCTTAATCCCC-3', (d) red emitters created in 5'-CCTCCTTCCTCC-3', (e) near-IR emitters created in 5'CCCTAACTCCCC-3', (f) emissive solutions. Figures are adapted from ref.(*37*)

Mass spectroscopy

Since synthesized DNA used in silver nanocluster preparation show monodispersity, mass spectrometry is another good method to characterize silver nanoclusters, as well as optical spectra. Generally, a mass spectrometer convert chemical compounds into charged molecules or fragments first. Then these ionized chemicals can shift with the help of external electric or magnetic field. Finally, it separates ions and measures the mass-to-charge ratios.

Petty and his group tried to characterize the silver nanocluster binding mode and sizes with mass spectra. In 2003, they investigated the silver nanoclusters trapped on the 12-base oligonucleotide (5'-AGGTCGCCGCCC-3')(*32*). In order to reduce the concentration of disturbing cations, the experiments was taken in water. The ratio of Ag^{+1}: oligonucleotide is 6:1. However, the spectra indicated that the most favorable complex is attached with 4 Ag^{+1} per strand. Unfortunately, according to a Poisson distribution, they could get the same result which makes it difficult to get a conclusion that complexes with more than four silver atoms are less stable. So they used some other sequences to check time evolution mass spectra. With a longer time, the distribution shift to a higher mass and end at 4Ag per strand, which is different from a Poisson distribution (Figure 11). There is a possibility that both the ion and metal complexes stoichiometries are the reason for the "end effects". Later, in 2007, they conducted mass spctra of silver clusters trapped in 12-mer polycystosine (dC12)(*33*). In this investigation, in addition to the spectrum showing the 6 Ag^{+1}:1 oligonucleotide as previous, they collected a spectrum showing 10-12 Ag^{+1}. In this spectrum, there are also a lot of Na^+ adducts, which lead them into a further study about the argument that metal ions can mediate cross-linking between bases(Figure 12). Mass spectra always fail to tell the difference between single clusters and several small clusters bound together to a single oligonucleotide. A systematic study on DNA with various lengths and sequences may bring some answers to this question.

22
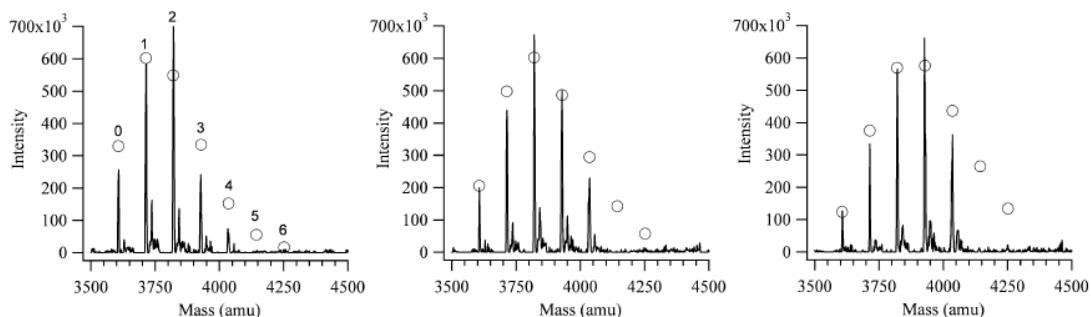
Figure 11 Electrospray ionization mass spectra of silver cluster complexes with the DNA oligonucleotide. Figure adapted from ref.(*32*)
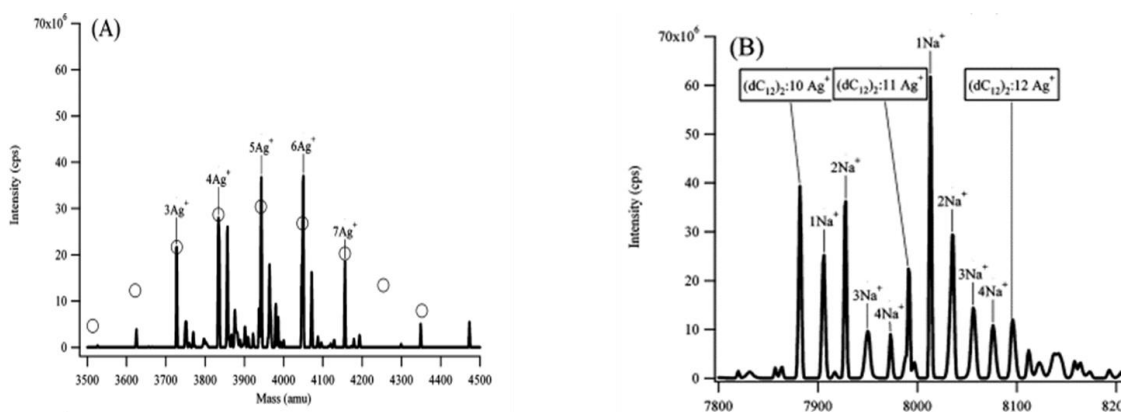
Figure 12 Electrospray ionization mass spectra of the dC$_{12}$: Ag$^+$ complexes. (A) the spectrum of the silver complexes with single-stranded dC$_{12}$ (B) the Na$^+$ adducts associated with each dC$_{12}$: Ag$^+$ complexes is indicated by the text in the box.

Current Applications

Take the advantage of ultra-small size and nontoxicity, AgNCs can be used for cell staining. Generally, ssDNA scaffold is supposed to provide a reaction site for biological molecules while stabilizing the emissive silver nanoclusters. Dickson et al. first used avidin-C$_{24}$-Ag NCs to produce high fluorescence intensity in cells(*34*). Later, antibody

DNA-Ag NC conjugate is also found to be attached to cell surface by antibody-antigen interaction(*34*).

Another application of silver nanoclusters is to detect metal ions. Wang's group is the first to detect Hg^{2+} whose concentration is in the range of 5nM to 1.5µM(*38*). With the presence of Hg^{2+} at some certain concentration, there is an obvious fluorescence quench. At the same time, when mixed with other metal ions, including Co^{2+}, Ni^{2+}, Pb^{2+}, Zn^{2+}, Cu^{2+}, Fe^{2+}, Fe^{3+}, Mn^{2+} and Cd^{2+},no such obvious phenomenon is observed. Chang's group established a "turn-on" method to detect Cu^{2+} (*39*).The fluorescence of DNA-Ag NCs increased when Cu^{2+} ion is introduced. Later, they developed another similar method. They quench the fluorescence of DNA-Cu/Ag NCs with 3-mercaptopropionic acid (MPA), and then the fluorescence recovered with the help of Cu^{2+}(*40*). In the range from 2nM to 200 nM, the higher the Cu^{2+} concentration is, the higher the fluorescence intensity is. With the presence of other metal ions, such as Zn^{2+}, Cd^{2+}, Pb^{2+}, Mg^{2+}, Mn^{2+}, Sr^{2+}, Hg^{2+}, Ni^{2+}, Co^{2+}, Ca^{2+}, Ag^+, Fe^{3+}, Al^{3+}, Cr^{3+}, no change of fluorescence intensity was found. In addition, the "Cu^{2+} effect" is not disturbed by the presence of Na^+, K^+, Mg^{2+}, Ca^{2+}, Zn^{2+}, Pb^{2+}, Cd^{2+}, Ni^{2+}, Cr^{2+} and Fe^{3+}. In this way, DNA-Ag NCs are thought selective to Hg^{2+} and Cu^{2+}.

The most interesting and challenging application of fluorescent silver nanoclusters is to detect biothiols, DNA, or proteins. Qu's group combined biothiols compounds with DNA-Ag NCs(*41*), and they found the change of the fluorescence is really sequence dependent. They indicated a "turn-on" study to detect cysteine base. Another strategy that

is widely studied is to use DNA-C$_{12}$-Ag NCs to detect specific target DNA sequences or identify mismatched base pairs. Martinez's group developed a method of using aptamer-DNA-Ag NCs to detect thrombin(*42*).

1.2.5 Other scaffolds

Some other scaffolds have been reported to stabilize silver nanoclusters. Silver clusters at sub-nanoscale has been successfully prepared on the interfaces of microemulsions(*43*). Chemical reduction with sodium borohydride is not the only way to reduce silver ions. Photogenerated ketyl radicals can reduce silver ions as well and aliphatic amines can stabilize the silver clusters. For instance, ketyl radicals decomposed from 2-hydroxy-1-(4-(2-hydroxyethoxy) phenyl)-2-methyl-1-propanone in an organic environment reduces silver ions to form silver nanoclusters, which are stabilized by cyclohexylamine(*44*). Thiol is also another popular chelating groups in synthesis of silver nanoparticles or nanoclusters(*45*).

Chapter 2 Experimental

The high tunability of the DNA sequences provides another degree of freedom for controlling the fluorescence properties. However, how DNA sequences and concentrations are modifying the photophysical properties have not been studied systematically. Here we provide a DNA sequence, concentration, and aging temperature dependent analysis of the florescent properties of silver nanoclusters.

2.1 Materials

We have used following materials without additional purification: silver nitrate (Aldrich, 99.998%), sodium borohydride (Fisher, 98%), ammonium acetate (Aldrich, 99.998%), Milli-Q water, and single-stranded DNA (IDT, PAGE purification or standard desalting as indicated in the text). DNA sequences are provided in the table.

Table 1 Description of sequences

Name	Sequence (5'-3')
D1	CCC TTA ATC CCC
D1'	GGG GAT TAA GGG
D2	CCC TCT TAA CCC
D3	CAT ACT TGA ACT T**CC CTT AAT CCC C**AA GTT CAA GTA TG

|	
D3'	CAT ACT TGA ACT TGG GGA TTA AGG GAA GTT CAA GTA TG
D4	CGG CAA AAG CCG
D5	CGG CGA AAG CCG

2.2 Synthesis

Based on the previous results others have got, we set the Ag: DNA ratio to be 1:3, and synthesis was carried out at the following concentrations:

$AgNO_3(\mu M)$	$DNA(\mu M)$	$NaBH_4(\mu M)$
160	480	160

1) Prepare 50µL ammonium acetate (10mM)

2) Prepare 10mM $AgNO_3$/buffer solution

3) Add 12µL $AgNO_3$ solution (10mM) to 20 µL DNA solution (1mM), and then add 93µL buffer into the tube. Keep the tube in dark at 4°C for 1 hour.

4) Prepare around 2mL $NaBH_4$/ cold H_2O solution (100mM).

5) Add 9.8µL $NaBH_4$ solution (10mM) to 990.8µL cold buffer in stock. Add 125µL diluted $NaBH_4$ solution to the tube above. The immediate interaction between $NaBH_4$ and H_2O takes place even at a very low temperature (<4°C). Hydrogen produced is this process make some air bubbles attached on the tube.

6) Keep the tube at room temperature in dark for one hour. In this process, the solution color changes gradually from transparent to light yellow or light pink.(Figure 13)
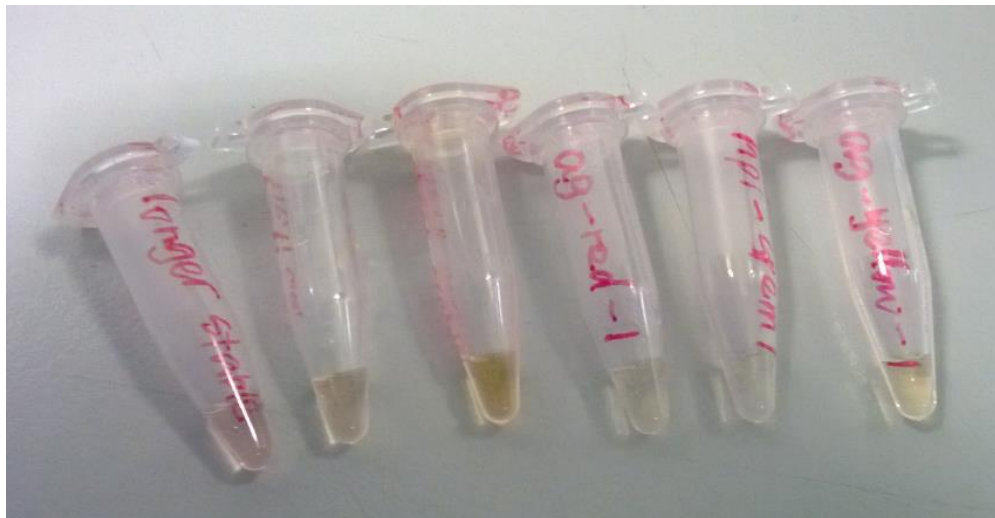
Figure 13 Silver nanocluster solution

2.3 Measurement

2.3.1 UV-vis measurement

UV-Vis spectra were collected at room temperature using PerkinElmer Lambda 25 spectrophotometer. For the typical measurements the samples after synthesis were diluted five times by mixing 50 µL of sample with 200 µL 10mM ammonium acetate buffer. The spectra were collected in 300 to 600nm range.

.

2.3.2 Fluorescence measurement

The fluorescence of silver nanolcusters are measured with ISS PC1 spectrofluorometer equipped with a temperature controlled cell holder. We used 1

mm slits for emission and excitation and the spectra were corrected for the instrumental response. In the typical measurements, 95 µL of stock sample after synthesis was diluted with 1400µL 40mM ammonium acetate for measurement. The measurement were performed at 20°C unless a different temperature is indicated. For all samples 400nm-800nm spectral range was investigated to identify fluorescent species at excitation and emission bands.

Fluorescence intensities are normalized with raman peak of water resonance in ammonium acetate buffer or corresponding intensities in excitation spectra. In my project, there are two scenario for normalization. When the raman peak of water can be separated completely with fluorescence peak, we normalized the data with the raman peak of water in silver nanocluster solution. When the raman peak of water partially or completely overlap with fluorescence peak, we measures the raman peak of water resonance in ammonium acetate buffer (40mM) immediately after the measurement of silver nanocluster by changing the sample chamber automatically. With normalization, the actual measurement condition is modified as an ideal one as following, 1)the light source must yield a constant photon output at all wavelengths; 2) the monochromator must pass photons of all wavelengths with equal efficiency; 3) the detector must detect photons of all wavelengths with equal efficiency. Normalized data are comparable at different excitation wavelengths, taking systematic noisy signals into consideration

Chapter 3 Cluster stability and post synthetic sample aging

The purpose of this experiment is to find an optimum synthesis condition and select proper sequences for further study which will be mentioned later in this thesis. In this study, we checked the following five different DNA sequences, D1, D2, D3, D4 and D5. Samples are prepared as the procedure described in Chapter 2, and then they were kept at different temperatures overnight. In addition, two of them (D1 and D2) were measured after a period time for a stability check. The UV-vis measurement and fluorescence measurement are taken as mentioned in Chapter 2.

Since there is a difference between excitation spectrum and UV-vis spectrum (Figure 15, Figure 16), we believe not all the species contained in the solution have fluorescence. In addition, there is a possibility that there may be some silver nanoparticles contained in the sample which have no fluorescence. However, the UV-vis spectrum measured after centrifugation (Figure 18) shows no difference before and after overnight centrifugation, which means there is no significant amount of nanoparticles (>2 nm) contained in the solution.

Silver nanoclusters templated on D1 contain two emitters or more which correspond to the two obvious peaks, and aging at 45℃ brings a fluorescence-stronger and spectrum-

purer sample (Figure 14, Figure 15). However, compared with 40°C, aging at 45°C caused a shorter-time stability (Figure 17). The different position of fluorescence excitation peak and UV-vis absorption peak suggests that not all the species contained in the sample are fluorescence emitters. Similar results can be observed in D3, the only thing different is that D1 sample had relatively cleaner UV-vis spectra at the beginning. However, the changes in Ag NCs trapped in D4 and D5 are another stories. The fluorescence was quenched a lot after aging at a temperature higher than 40°C, although the structures were more uniform than aging at a temperature lower than 35°C (Figure 21). For D2, aging at 50°C gives a more stable and fluorescence-stronger sample.
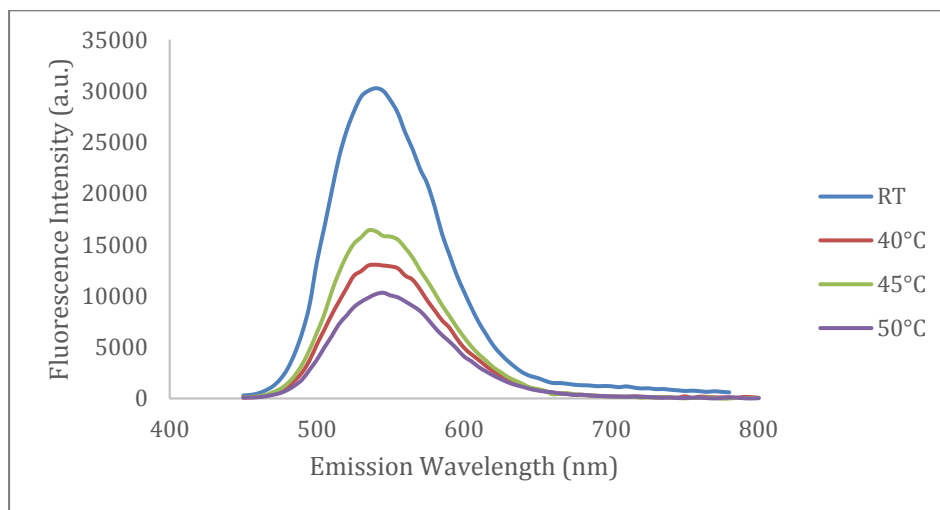
Figure 14 Fluorescence emission spectrum of D1-templated silver nanoclusters. The samples aged overnight at room temperature (23 ℃), 40 ℃, 45 ℃ and 50 ℃.
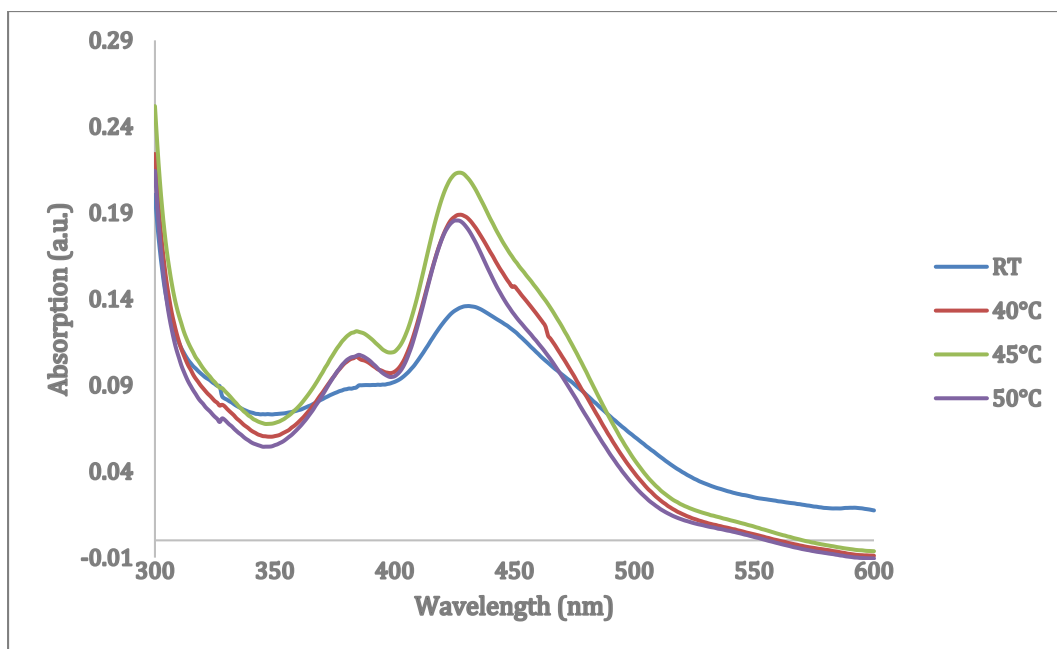
Figure 15 UV-vis spectrum of D1-templated silver nanoclusters. The samples aged overnight at room temperature (23 ℃), 40 ℃, 45 ℃ and 50 ℃.
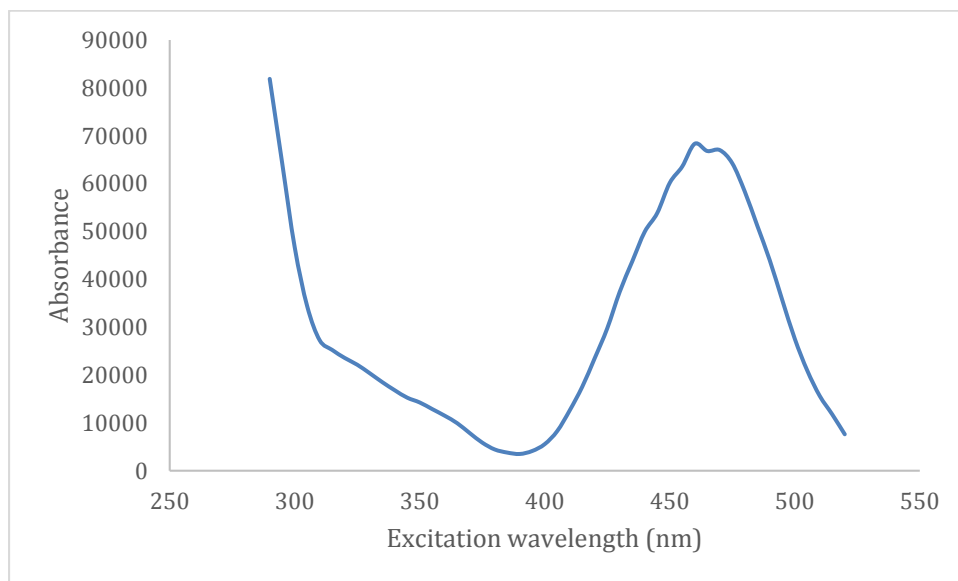
Figure 16 Excitation spectrum of D1-templated silver nanoclusters at room temperature (22 ℃)

Figure 17 Fluorescence emission spectrum of D1-templated silver nanoclusters. After overnight aging at room temperature (23 ℃), 40 ℃, 45 ℃ and 50 ℃, samples were measured 1 day,, 3days and 7days later.

Figure 18 UV-vis spectrum of D1-templated silver nanoclusters. The samples aged overnight at room temperature after centrifugation.
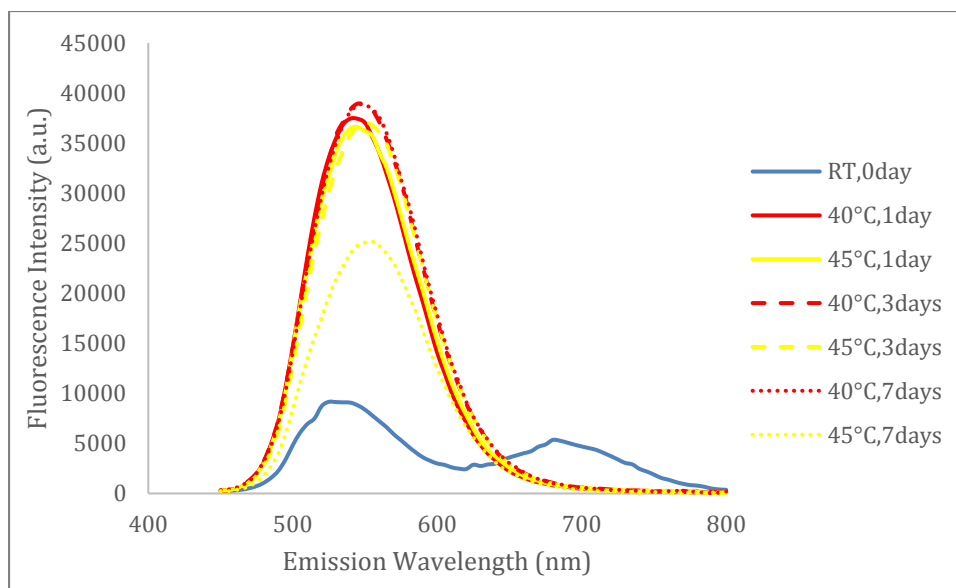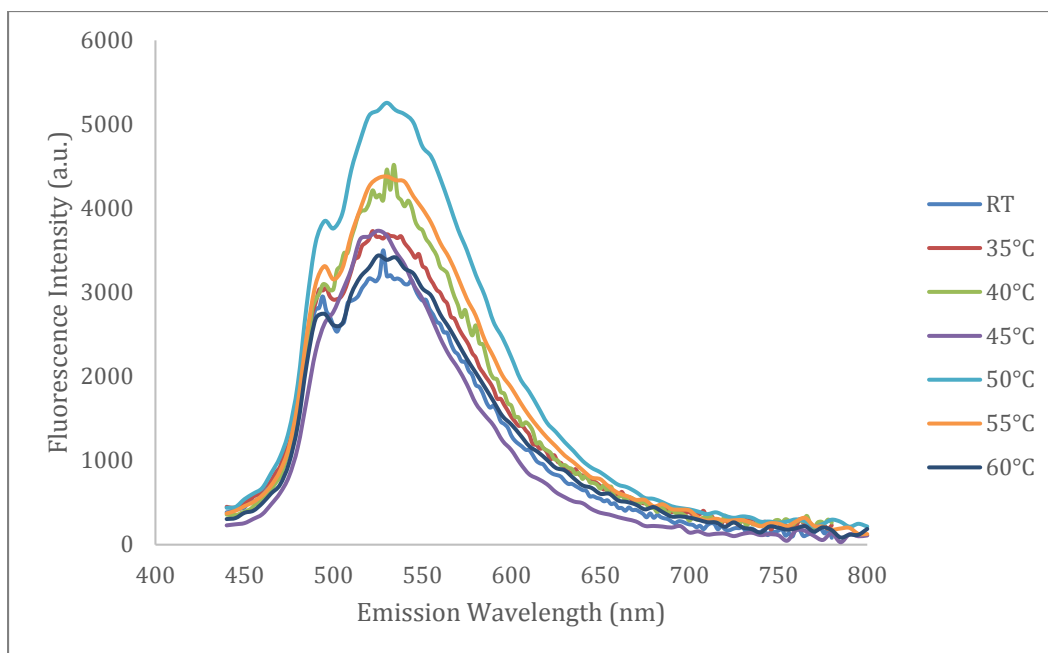
Figure 19 Fluorescence emission spectrum of D3-templated silver nanoclusters. The samples aged overnight at room temperature (23 ℃), 35 ℃, 40 ℃, 45 ℃, 50 ℃, 55 ℃ and 60 ℃.
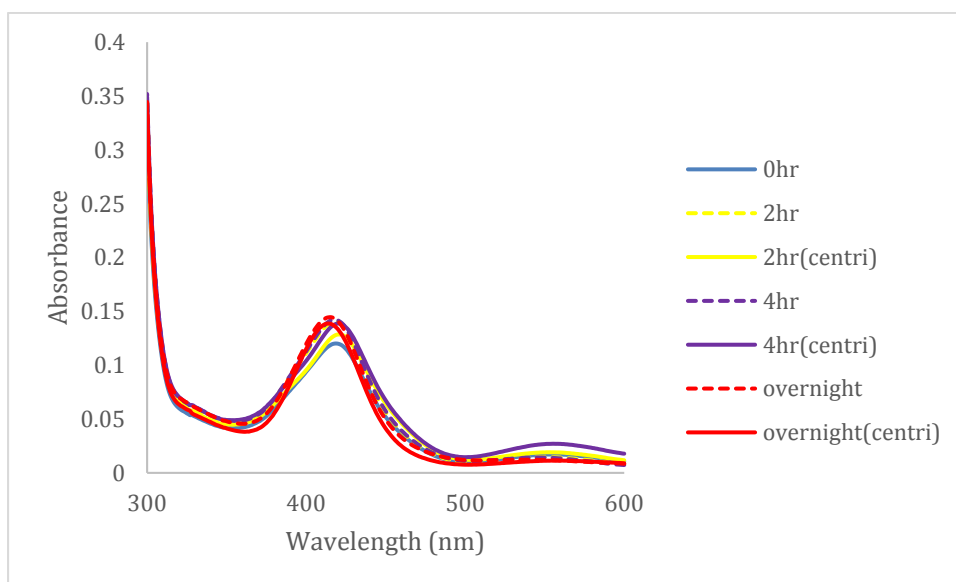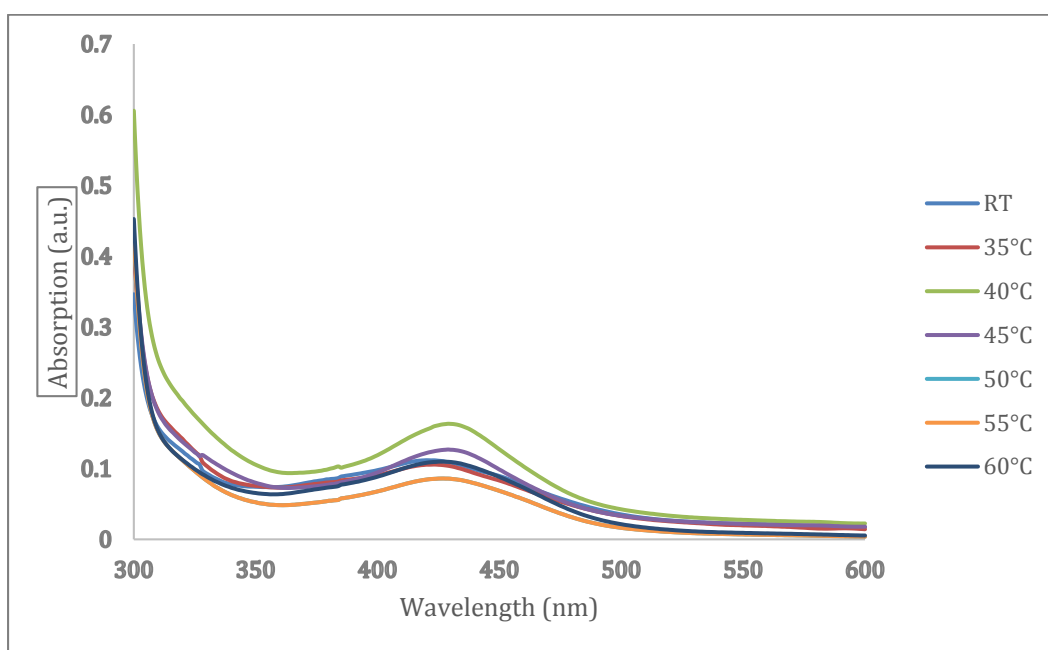

Figure 20 UV-vis spectrum of D3-templated silver nanoclusters. The samples aged overnight at room temperature (23 ℃), 35 ℃, 40 ℃, 45 ℃, 50 ℃, 55 ℃ and 60 ℃.
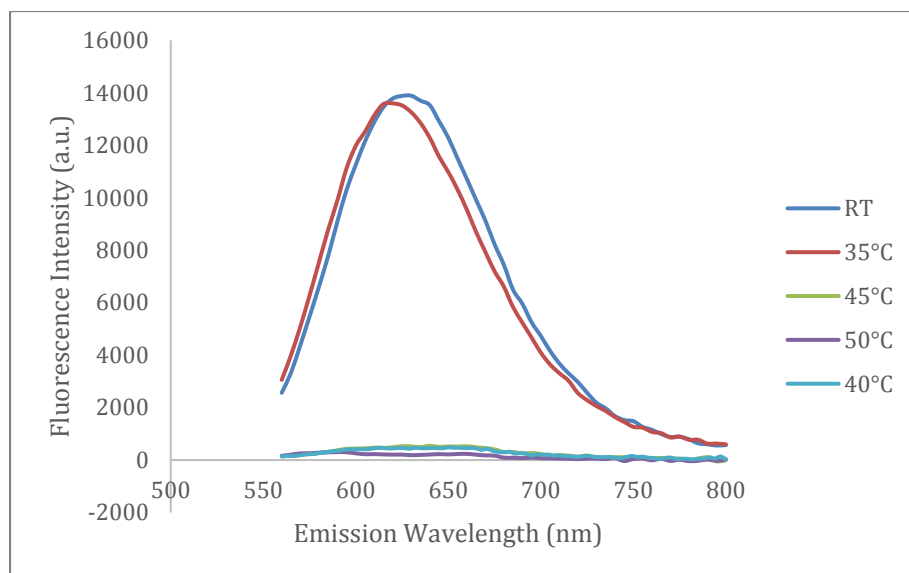
Figure 21 Fluorescence emission spectrum of D4-templated silver nanoclusters. The samples aged overnight at room temperature (23 ℃), 35 ℃, 40 ℃, 45 ℃ and 50 ℃.

Figure 22 UV-vis spectrum of D4-templated silver nanolcusters. The samples aged overnight at room temperature (23 ℃), 35 ℃, 40 ℃, 45 ℃ and 50 ℃.
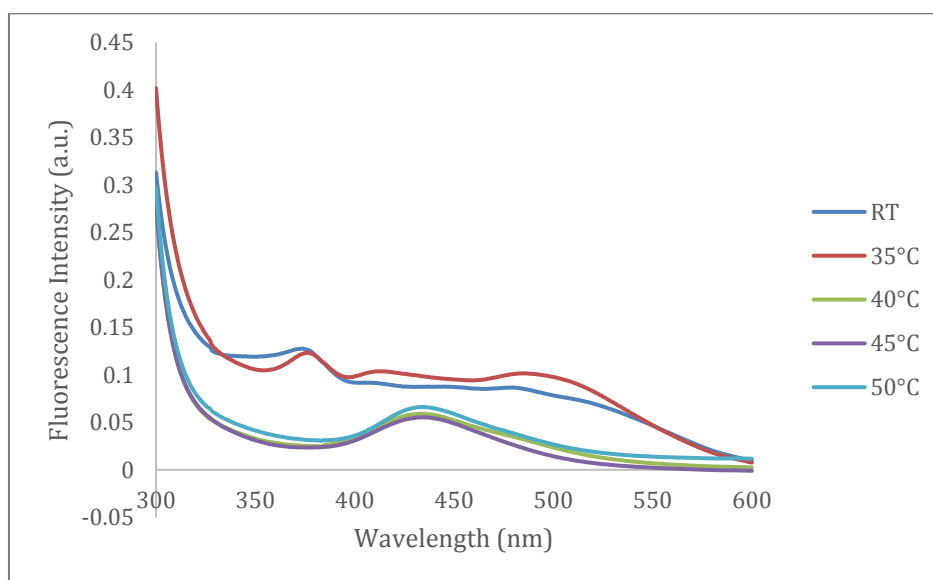
Based on the results above we got, there is not a fixed optimum aging temperature for silver nanoclusters, that is to say, it is sequence dependent. Both nucleotide bases and the

length of sequences can be the affecting factors. Aging temperatures may affect not only the binding between DNA sequences and silver atoms, but also the binding between nucleotide bases, which partially determine the secondary structure of DNA sequences. All these factors are potential directions that is worth being studied further.

Out of five sequences, we have chosen D1 and D3 aged at 40°C and 50°C for further concentration dependence and sequence dependence studies, since they show more uniform absorbence and emission spectra, which implies more uniform structure, and show stable fluorescence signal over time.

# Chapter 4 DNA concentration effect on AgNCs fluorescence

In this experiment, we used a DNA sequence D3, which has a hairpin secondary structure, (5'- CAT ACT TGA ACT TCC CTT AAT CCC CAA GTT CAA GTA TG-3') and D1 (5'-CCC TTA ATC CCC-3') as scaffolds which shows good stability over time and single fluorescence emission peak. Previous studies (33, 35) indicate that changing Ag to DNA ratio in a synthesis mixture significantly affects the spectral signature of the resulting AgNCs solution. In this case, change in the spectral properties could be due to both change of Ag cluster structure itself during the synthesis step or due to change in the DNA environment. To investigate this problem we designed the experiment where concentration of stabilizing DNA is changed after the AgNC synthesis. In this case, the cluster is already synthesized and any possible changes in the properties of the AgNCs with post synthetic addition of DNA would only due to the change in the stabilizing environment of the DNA shell. Sample in this experiment was prepared in the procedure described in Chapter 2, and then sample was aged at the specified temperature overnight. After aging, sample was diluted as indicated in Chapter 2 - 95μL of sample mixed with 1400μL of buffer (ammonium acetate, 40mM) right before fluorescence measurements. The spectra were taken every 10 minutes on a 40 minutes time interval, then the DNA concentration was increased by adding extra DNA solution (1mM) to the sample and carefully mixing. The 40 min time interval was chosen experimentally, as the time

necessary for fluorescence reading to stabilize after DNA addition. To account for dilution effects, sample aging and instrumental drift, we have measured fluorescence of the control sample which was equivalent to the sample of interest with the only difference that instead of DNA we have added same volume of the buffer (ammonium acetate, 40mM).

The fluorescence of Ag NCs synthesized with D3 was evidently enhanced with the increase of D3 DNA concentration up to 40µM, then the fluorescence was quenched to the value of the control sample (Figure 23, Figure 24). At the same time, there was a slight blue shift as well as appearance of a shoulder at longer emission wavelength. In the case of D1, there was a more complicated phenomenon. The initial fluorescence of a green emitter was quenched with the increase of D1 concentration, and the fluorescence of a red emitter increased first, reaching maximum at about 20µM, and then decreased (Figure 25, Figure 26). A large blue shift occurred in the red region as well.
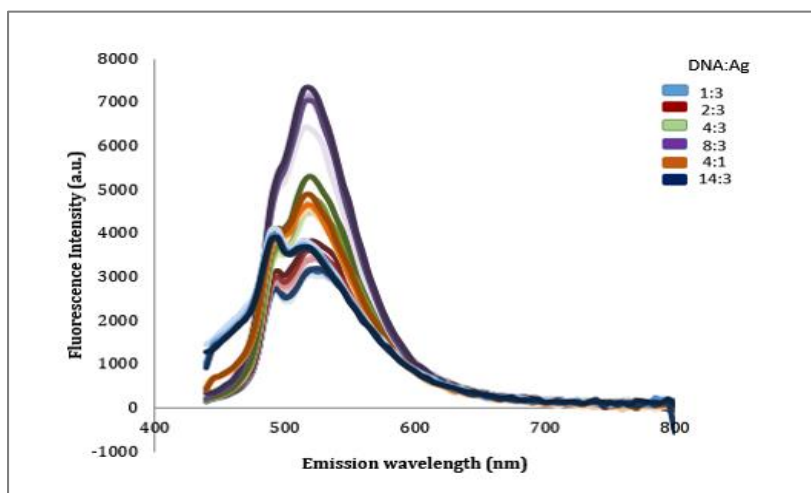
Figure 23 Fluorescence emission spectrum of D3-templated silver nanoclusters. During measurement, excess standard desalted D4 solution was added to the sample. For each Ag:DNA ratio, the sample was measured every 10 minutes within 40minutes.

38
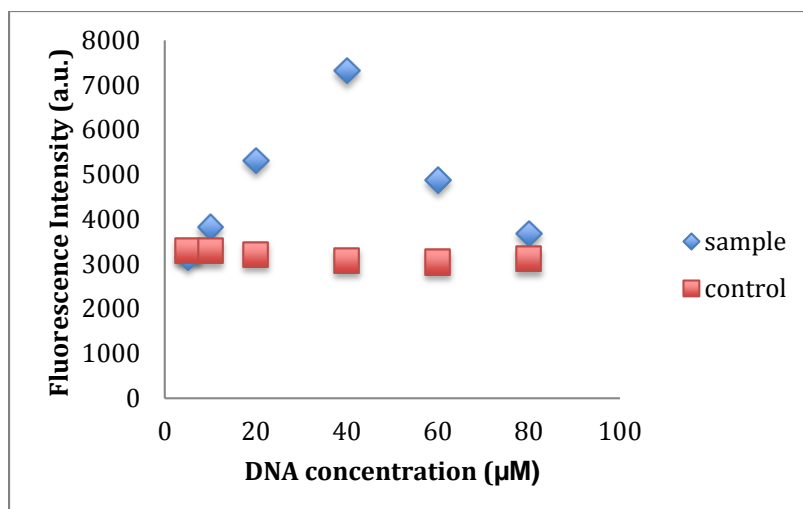
Figure 24 Change of peak fluorescence intensity of D3-templated silver nanolusters. Control sample was added with the same volume of ammonium acetate buffer as extra D3 solution.
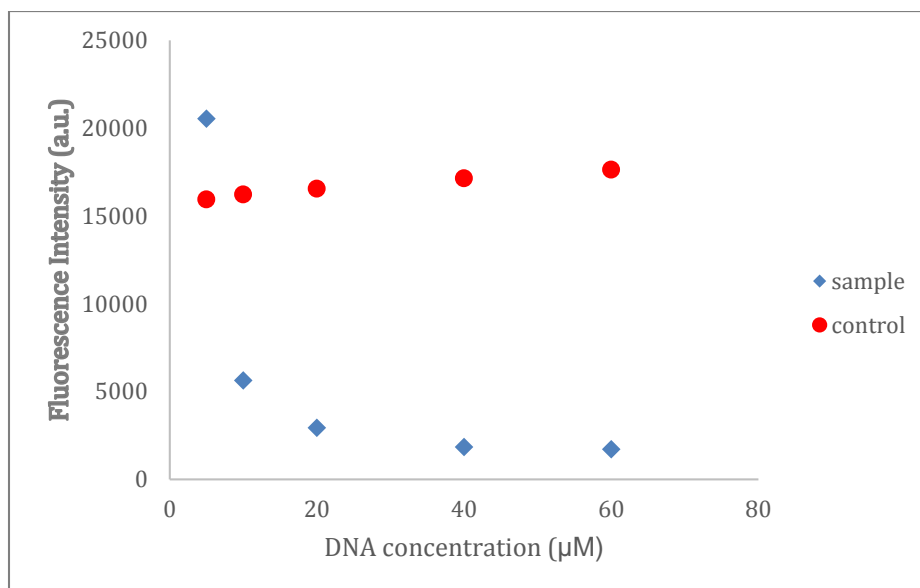

Figure 25 Fluorescence emission spectrum of D1-templated silver nanoclusters. During measurement, excessive standard desalted D1 solution was added to the sample. For each Ag:DNA ratio, the sample was measured every 15 minutes within an hour

Figure 26 Change of peak fluorescence intensity of D3-templated silver nanoclusters. Control sample was added with the same volume of ammonium acetate buffer as extra D3 solution.

The observed effect of DNA concentration on the AgNCs is somewhat surprising. There is a great difference between the tendency in AgNCs synthesized with hairpin sequence (D3) and linear sequence (D1). Via comparing two control samples, taking consideration of sequence secondary structure, a hairpin structure (D3) is more capable in stabilizing AgNCs than a linear structure (D3), which brings a more constant fluorescence intensity. At the same time, when in terms of nucleotide bases, silver nanoclusters in a cytosine-rich sequence are more likely to be stronger emitters. Although, hairpin sequence templated silver nanoclusters show much weaker fluorescence initially, with the DNA concentration increases, the fluorescence is enhanced first and then quenched. This watershed is probably due to the saturation of silver binding with DNAs, which is an equilibrium status of the whole system. For a linear sequence, the fluorescence intensity

evidently decreases by adding excessive DNA solution. With more DNA, the stable

bonds between Ag and N3 on cytosine can be disrupted, since some other hydrogen

bonds between DNA side chains or backbones can be set up. However, whether these

phenomena and inferences are sequence selective or not is still unknown yet.

Chapter 5 Sequence dependence studies

In this experiment, samples were prepared with the same DNAs in the same procedure as before. The difference in this experiment is that we added the various sequences to the diluted sample for measuring. We added D4 (5'-CGG CAA AAG CCG-3') and D5 (5'-CGG CGA AAG CCG-3') to both of the two samples. What's more, we added complimentary sequences to each of the two samples. The purpose of this experiment is to try to find out how the sequences have an impact on the change of fluorescence intensities.

In both of the two cases, compared to other sequences, D6 and D7 can largely reduce the peak shift while excessive DNA is added. The other sequences all bring more or less blue shifts of the fluorescence peaks. Additional DNA solutions enhance the red-emissive fluorescence of silver nanoclusters in D1, and in opposite, the green-emissive fluorescence is quenched (Figure 29, Figure 31, Figure 32). In the case of D3 templated silver nanoclusters, only D3 and D3 complimentary bring an enhancement in the fluorescence intensity, and the other two sequences bring a decrease of fluorescence intensities (Figure 27, Figure 28, Figure 30).

Figure 27 Change of peak fluorescence wavelengths of D3-templated silver nanoclusters with extra other DNA solutions

Figure 28 Change of peak fluorescence intensities of D3-templated silver nanoclusters with extra other DNA solutions

Figure 29 Change of peak fluorescence intensities of D1-templated silver nanoclusters with extra other DNA solutions in green emission region.

Figure 30 Change of peak fluorescence wavelengths of D1-templated silver nanoclusters with extra other DNA solutions in green emission region.

Figure 31 Change of peak fluorescence intensities of D1-templated silver nanoclusters with extra other DNA solutions in red emission region.

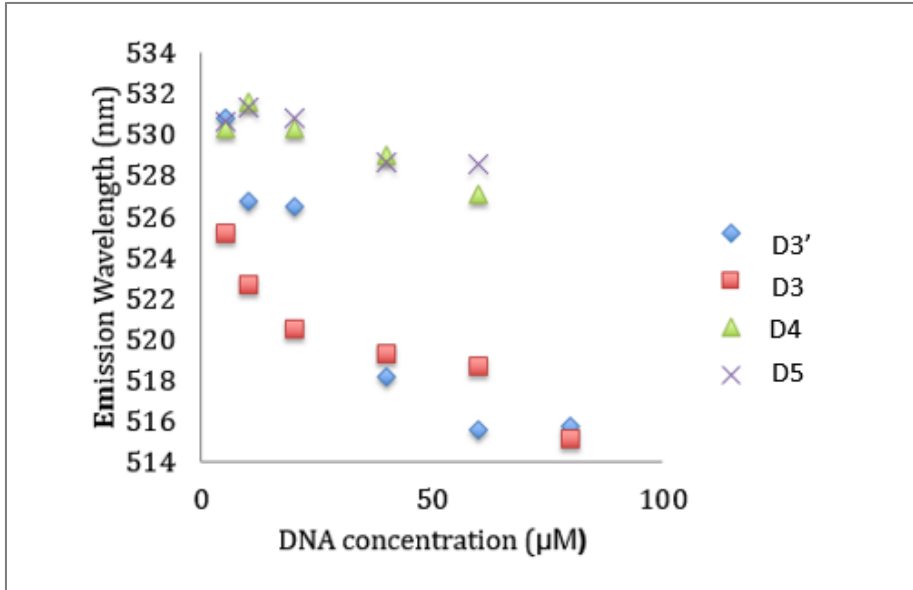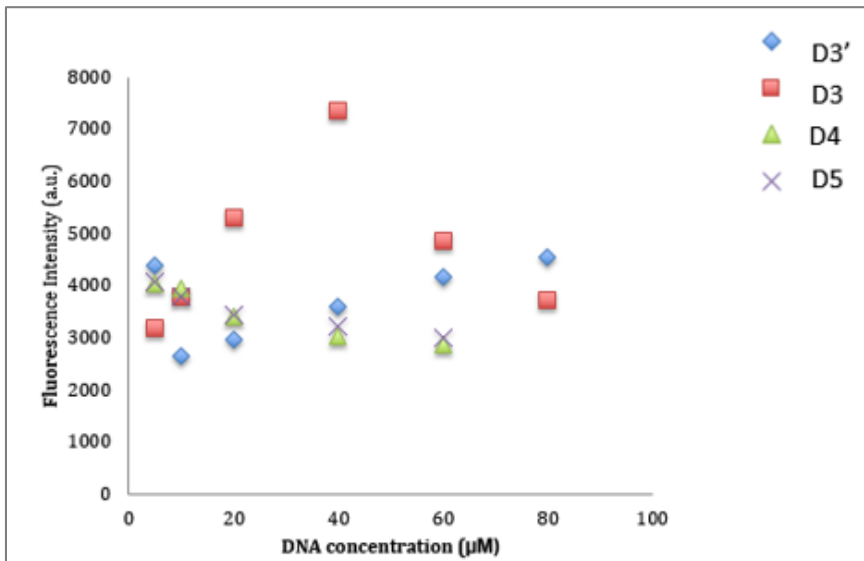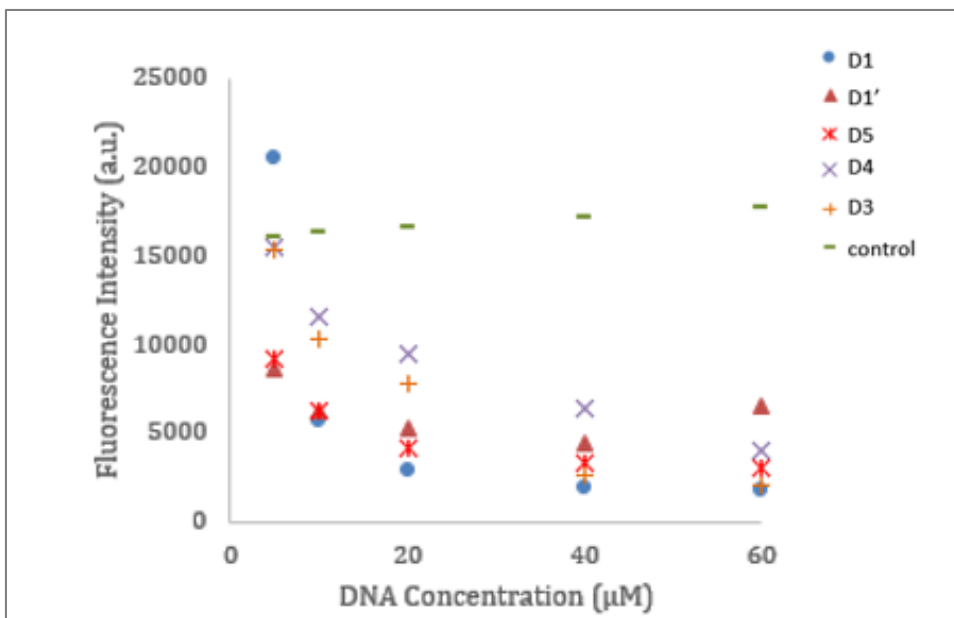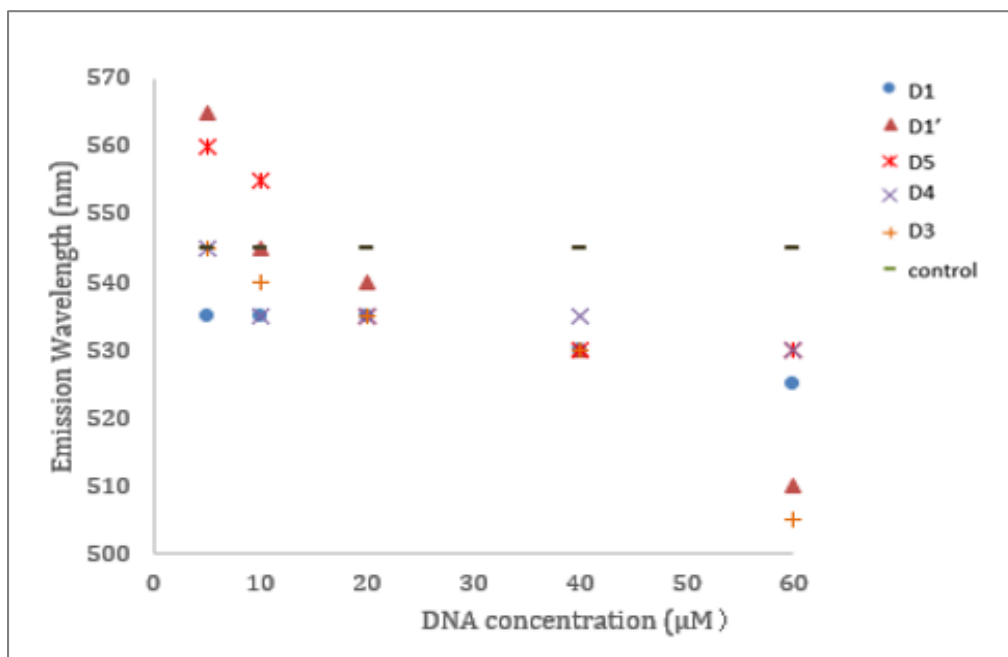**Figure 32 Change of peak fluorescence wavelengths of D1-templated silver nanoclusters with extra other DNA solutions in red emission region.**
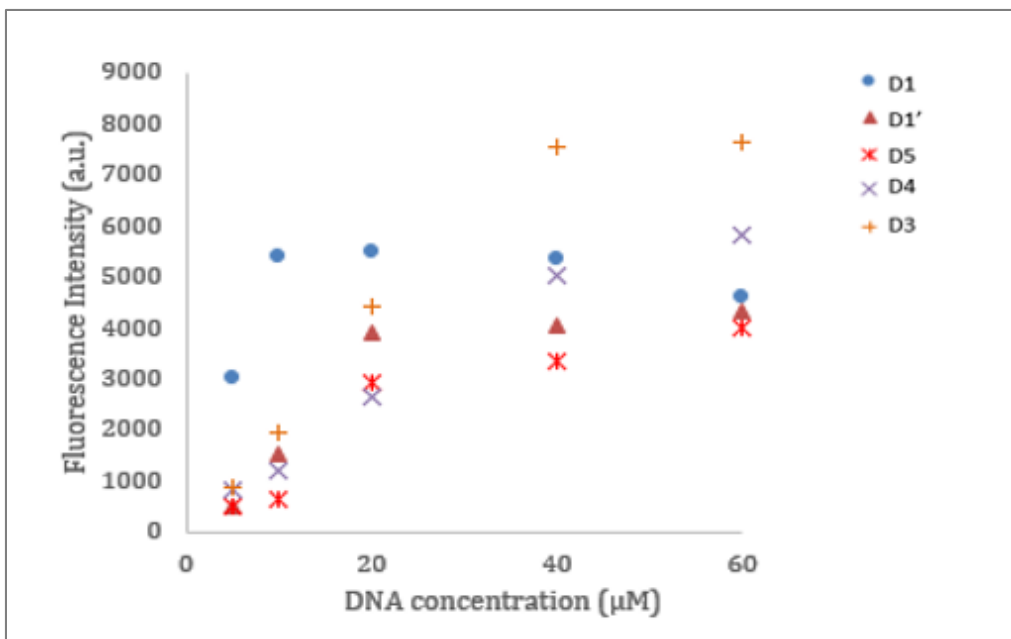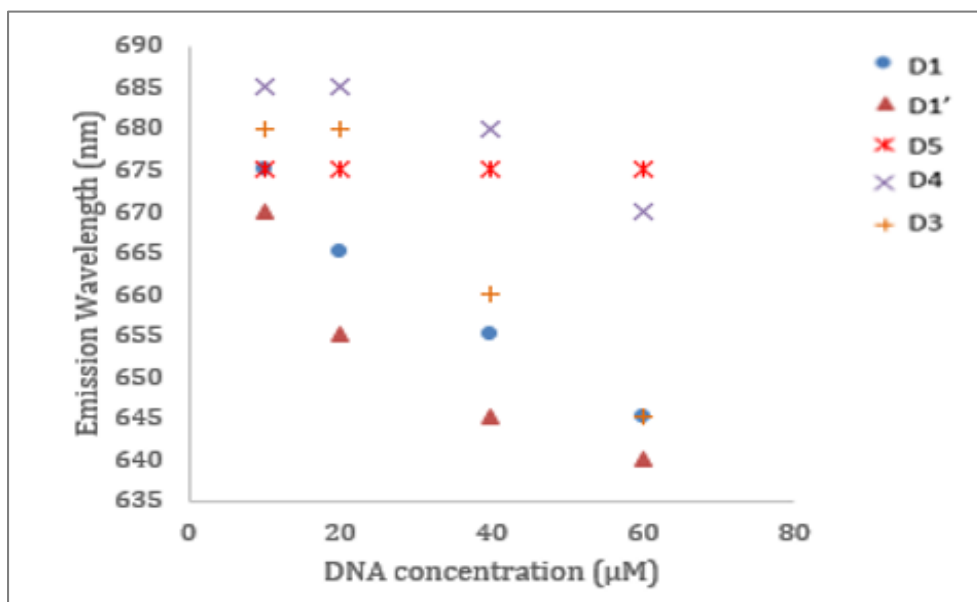
The tendency of the change of fluorescence may highly depend on the specific DNA sequences involved in tuning. When AgNCs are trapped in hairpin DNA sequences, only

45

adding hairpin DNA sequences can enhance the fluorescence of the clusters. The reason for this may be due to the relatively inflexible secondary structure of these DNA sequences make the combination between Ag and DNA more stable. With adding more and more DNA solution, the spare silver clusters tend to be wrapped completely. And after a complete wrapping, the fluorescence intensity tend to be stable or decrease with the dilution of the silver clusters concentration. An interesting turning point in the D4 complimentary curve is at 10μM, at which the ratio between additional D4 complementary DNA and D4 is 1:1. This characteristic point may be the result of the "zip" formed by the two complimentary DNA sequences. This critical point is a good potential choice for a hairpin specific probe.

In D5 based AgNCs, all the additional DNA sequences make a decrease of the green-emissive fluorescence and an increase of red-emissive fluorescence. Since there is a partial overlap in the emission spectrum and excitation spectrum of these two emitters, this phenomenon is so called fluorescence resonance energy transfer (FRET), in which process the donor and acceptor are coupled by a dipole-dipole interaction. An interesting tendency in D5 curve is that when the ratio between DNA and Ag is larger than 2:3, the fluorescence intensity tends to be constant which may correspond to the saturation status of silver clusters.

However, whether these conclusions secondary structure dependent or sequence length dependent has not been known yet, which need further studies based on more different DNA sequences.

Chapter 6 Future Outlooks

The synthesis and characterization of some specific DNA-templated silver nanoclusters have been summarized in this thesis. DNA-templated silver nanoclusters are DNA tunable and show a good fluorescence property. Despite different oligonucleotide sequences and conformation have been used to synthesize Ag NCs, we still cannot clearly elaborate the interaction mechanism between silver clusters and DNA sequences.

Now that silver nanoclusters have good biocompatibility, it is quite worthy for us to move on a further step in the study of silver nanolcuster application. In the future, we plan to get a more precise and refined study in complimentary DNA sequences detection, especially when the ratio between two sequences is less than 1:1. On the other hand, we plan to synthesis silver nanoclusters in different pH conditions, which will give some hint about the synthesis mechanism. Also, different pH condition may provide silver nanoclusters that can be applied in different biochemical environments, where a bright future can be expected.

Reference

1. T. Schmidt, U. Kubitscheck, D. Rohler, U. Nienhaus, *Single Molecules* **3**, 327 (2002).

2. K. A. Willets, O. Ostroverkhova, M. He, R. J. Twieg, W. E. Moerner, *Journal of the American Chemical Society* **125**, 1174 (2003/02/01, 2003).

3. W. G. J. H. M. van Sark *et al.*, *The Journal of Physical Chemistry B* **105**, 8281 (2001/09/01, 2001).

4. C. Félix *et al.*, *Physical Review Letters* **86**, 2992 (2001).

5. S. A. Blanton, A. Dehestani, P. C. Lin, P. Guyot-Sionnest, *Chemical Physics Letters* **229**, 317 (1994).

6. M. Nirmal *et al.*, *Nature* **383**, 802 (Oct 31, 1996).

7. J. P. Wilcoxon, B. L. Abrams, *Chemical Society Reviews* **35**, 1162 (2006).

8. X. Lu, M. Rycenga, S. E. Skrabalak, B. Wiley, Y. Xia, *Annual Review of Physical Chemistry* **60**, 167 (2009).

9. L. Brewer, B. A. King, J. L. Wang, B. Meyer, G. F. Moore, *The Journal of Chemical Physics* **49**, 5209 (1968).

10. V. K. Tikhomirov *et al.*, *Opt. Express* **18**, 22032 (2010/10/11, 2010).

11. G. De Cremer *et al.*, *Journal of the American Chemical Society* **131**, 3049 (2009/03/04, 2009).

12. S. Fedrigo, W. Harbich, J. Buttet, *The Journal of Chemical Physics* **99**, 5712 (1993).

13.   W. Harbich *et al.*, *The Journal of Chemical Physics* **93**, 8535 (1990).

14.   C. Félix *et al.*, *Chemical Physics Letters* **313**, 105 (1999).

15.   C. Félix *et al.*, *Physical Review Letters* **86**, 2992 (2001).

16.   R. S. Eachus, A. P. Marchetti, A. A. Muenter, *Annual Review of Physical Chemistry* **50**, 117 (1999).

17.   L. A. Peyser, A. E. Vinson, A. P. Bartko, R. M. Dickson, *Science* **291**, 103 (January 5, 2001, 2001).

18.   A. Henglein, *Chemical Physics Letters* **154**, 473 (1989).

19.   B. G. Ershov, A. Henglein, *The Journal of Physical Chemistry B* **102**, 10663 (1998/12/01, 1998).

20.   M. Mostafavi, N. Keghouche, M.-O. Delcourt, J. Belloni, *Chemical Physics Letters* **167**, 193 (1990).

21.   J. Zhang, S. Xu, E. Kumacheva, *Advanced Materials* **17**, 2336 (2005).

22.   Z. Shen, H. Duan, H. Frey, *Advanced Materials* **19**, 349 (2007).

23.   L. Shang, S. Dong, *Chemical Communications*, 1088 (2008).

24.   I. Díez *et al.*, *Angewandte Chemie International Edition* **48**, 2122 (2009).

25.   H. Xu, K. S. Suslick, *ACS Nano* **4**, 3209 (2010/06/22, 2010).

26.   N. Makarava, A. Parfenov, I. V. Baskakov, *Biophys J* **89**, 572 (2005).

27.   M. Lafarga, I. Casafont, R. Bengoechea, O. Tapia, M. Berciano, *Chromosoma* **118**, 437 (2009/08/01, 2009).

28.   J. Yu, S. Choi, R. M. Dickson, *Angewandte Chemie* **121**, 324 (2009).

29.   S. S. Narayanan, S. K. Pal, *The Journal of Physical Chemistry C* **112**, 4874 (2008/04/01, 2008).

30.   A. Ono, Y. Miyake, *Nucleic Acids Symposium Series* **3**, 227 (September 1, 2003, 2003).

31.   S. A. Patel, C. I. Richards, J.-C. Hsiang, R. M. Dickson, *Journal of the American Chemical Society* **130**, 11602 (2008/09/03, 2008).

32.   J. T. Petty, J. Zheng, N. V. Hud, R. M. Dickson, *Journal of the American Chemical Society* **126**, 5207 (2004/04/01, 2004).

33.   C. M. Ritchie *et al.*, *The Journal of Physical Chemistry C* **111**, 175 (2007/01/01, 2006).

34.   S. Choi, J. Yu, S. A. Patel, Y.-L. Tzeng, R. M. Dickson, *Photochemical & Photobiological Sciences* **10**, 109 (2011).

35.   J. Sharma, H.-C. Yeh, H. Yoo, J. H. Werner, J. S. Martinez, *Chemical Communications* **46**, 3280 (2010).

36.   E. G. Gwinn, P. O'Neill, A. J. Guerrero, D. Bouwmeester, D. K. Fygenson, *Advanced Materials* **20**, 279 (2008).

37.   C. I. Richards *et al.*, *Journal of the American Chemical Society* **130**, 5038 (2008/04/01, 2008).

38.   W. Guo, J. Yuan, Q. Dong, E. Wang, *Journal of the American Chemical Society* **132**, 932 (2010/01/27, 2009).

39.   G.-Y. Lan, C.-C. Huang, H.-T. Chang, *Chemical Communications* **46**, 1257 (2010).

40.   Y.-T. Su, G.-Y. Lan, W.-Y. Chen, H.-T. Chang, *Analytical Chemistry* **82**, 8566 (2010/10/15, 2010).

41.   Z. Huang, F. Pu, Y. Lin, J. Ren, X. Qu, *Chemical Communications* **47**, 3487 (2011).

42.   J. Sharma, H.-C. Yeh, H. Yoo, J. H. Werner, J. S. Martinez, *Chemical Communications* **47**, 2294 (2011).

43.   A. Ledo-Suárez *et al.*, *Angewandte Chemie International Edition* **46**, 8823 (2007).

44.   L. Maretti, P. S. Billone, Y. Liu, J. C. Scaiano, *Journal of the American Chemical Society* **131**, 13972 (2009/10/07, 2009).

45.   R. Jin, *Nanoscale* **2**, 343 (2010).